Bound states without potentials: Localization at singularities

Eric He[1,2,*] and R. Ganesh[2,†]
[1]*University of California, Berkeley, California 94720, USA*
[2]*Department of Physics, Brock University, St. Catharines, Ontario, Canada L2S 3A1*

(Received 13 February 2023; revised 15 July 2023; accepted 20 July 2023; published 4 August 2023)

Bound-state formation is a classic feature of quantum mechanics, where a particle localizes in the vicinity of an attractive potential. This is typically understood as the particle lowering its potential energy. In this article, we discuss a paradigm where bound states arise purely due to kinetic-energy considerations. This phenomenon occurs in certain nonmanifold spaces that consist of multiple smooth surfaces that intersect one another. The intersection region can be viewed as a singularity where dimensionality is not defined. We demonstrate this idea in a setting where a particle moves on M spaces ($M = 2, 3, 4, \ldots$), each of dimensionality D ($D = 1$, 2, and 3). The spaces intersect at a common point, which serves as a singularity. To study quantum behavior in this setting, we discretize space and adopt a tight-binding approach. We generically find a ground state that is localized around the singular point, bound by the kinetic energy of "shuttling" among the M surfaces. We draw a quantitative analogy between singularities on the one hand and local attractive potentials on the other. To each singularity, we assign an equivalent potential that produces the same bound state wave function and binding energy. The degree of a singularity M (the number of intersecting surfaces) determines the strength of the equivalent potential. With $D = 1$ and $D = 2$, we show that any singularity creates a bound state. This is analogous to the well-known fact that any attractive potential creates a bound state in one and two dimensions. In contrast, with $D = 3$, bound states appear only when the degree of the singularity exceeds a threshold value. This is analogous to the fact that in three dimensions, a threshold potential strength is required for bound-state formation. We discuss implications for experiments and theoretical studies in various domains of quantum physics.

DOI: 10.1103/PhysRevA.108.022202

I. INTRODUCTION

A free particle, in its quantum-mechanical ground state, typically spreads uniformly to occupy all available space. This allows the particle to lower its kinetic energy. However, in the presence of an attractive potential, it may localize into a bound state to lower its potential energy. This phenomenon reflects competition between kinetic and potential energies. In this article, we discuss a paradigm where bound states form without any potentials. Rather, the particle moves on a singular space consisting of multiple surfaces that intersect at a "junction." This allows for a new type of kinetic energy that favors localization of the particle. We present a detailed analysis of this phenomenon, focusing on the role of dimensionality.

Quantum mechanics on intersecting spaces is a concrete, testable proposition. Experiments with semiconductor architectures have explored X junctions and T junctions. Indeed, bound states have been seen where electrons or holes are localized near junctions [1–4]. Collective excitonic excitations have also been found to bind to junctions [5–8]. Analogous phenomena may also occur in classical wave mechanics, e.g., in junctions of photonic [9] or phononic waveguides [10,11]. Recently, singular spaces have been invoked to describe quantum magnets. At low energies, the physics of a quantum magnet resembles that of a particle moving on the space of classical ground states [12,13]. In certain magnetic clusters, frustration leads to complex spaces that contain intersecting wires and sheets. At very low energies, the magnet freezes at the intersection; that is, it orders in a particular classical configuration. This is equivalent to a particle binding to a junction due to bound-state formation. This effect has been called "order by singularity," a special case of the well-known order-by-disorder phenomenon [12–15]. In these various experimental settings, junctions induce bound states with dramatic physical consequences. The goal of this article is to develop an understanding of this phenomenon, its physical origin, and its organizing principles.

We consider a class of spaces consisting of multiple surfaces that intersect one another. The locus of intersection represents a singularity. In the discussion below, we characterize each singularity by two quantities: codimension and degree. Figure 1 shows some examples. In the left panel, we show three one-dimensional channels that intersect at a point-like junction. A generic point in this space lies on one of the channels; its local neighborhood is one-dimensional. In contrast, the junction is a zero-dimensional region (a point) whose local neighborhood does not have a well-defined dimensionality. The difference between these two dimensionalities is the codimension, which is unity here. In addition, we assign a degree of 3, representing the number of channels that meet at this junction. In the middle panel of Fig. 1, we see two

*heeric@berkeley.edu
†r.ganesh@brocku.ca

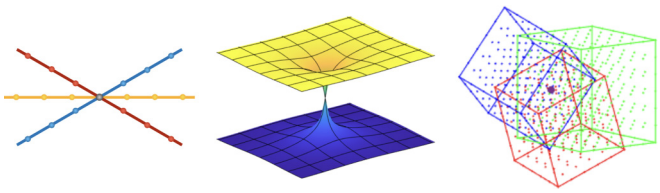

FIG. 1. Self-intersecting spaces. Left: Three wires (one-dimensional spaces) that intersect at a point. Middle: Two sheets (two-dimensional spaces) that intersect at a point. Right: Three cubes (three-dimensional spaces) that intersect at a point.

sheets that intersect at a point. This represents a singularity of codimension 2. The space is generically two-dimensional (2D), while the singularity is pointlike. As we have two sheets, the degree is 2. In the right panel of Fig. 1, we see three cubes which are understood to share a common point. The common point is a zero-dimensional singularity. The codimension and the degree are 3 in this case.

For comparison, we will also discuss bound states induced by attractive potentials on smooth spaces. There is extensive literature available on bound states induced by various potentials. It is well known that dimensionality plays a key role. In one and two dimensions, an infinitesimal potential suffices to create a bound state. However, in three and higher dimensions, a threshold potential strength is required [16–19]. In this article, we use a tight-binding approach that can handle both singularities and potentials on the same footing. Naively, the problem of a potential appears to be very different from that of a singularity. However, our results bring out a deep connection. As we show below, any singularity is quantitatively equivalent to a potential in the sense that it produces the same bound state.

II. THE TIGHT-BINDING APPROACH

The traditional approach to quantum mechanics is to construct a Hamiltonian operator and find its eigenfunctions. This cannot be carried out on singular spaces because the Hamiltonian cannot be written down in the vicinity of a singularity. For example, a gradient operator cannot be defined near a junction of two wires. Solutions can still be found using *ad hoc* methods. For example, eigenfunctions can be found on each smooth segment, with a suitable boundary condition imposed at the singularity. The choice of boundary condition can affect the result [20–22].

In this article, we take an alternative approach using tight binding. Originally developed to describe band structure in solids, tight binding typically describes an electron in a lattice of atoms [23–25]. The Hilbert space is spanned by localized wave functions centered on each atom. If the lattice constant is not too small, an electron hops from an atom to any of its neighbors. Here, we adapt this approach with "atoms" arranged on a singular space rather than forming a regular lattice.

The tight-binding approach lends itself to an ambiguity-free procedure for a one-dimensional problem, such as the one shown in Fig. 1 (left). In two dimensions and higher, there can be multiple ways of discretizing a smooth surface. For example, a smooth two-dimensional region can be discretized into a square or a triangular grid. Once this choice is made, there is no further ambiguity in the procedure or the solutions obtained. In our calculations, we choose a square (cubic) discretization for two (three) dimensions.

In the rest of this article, we solve free-particle tight-binding Hamiltonians of the form

$$H = -t \sum_{\langle mn \rangle} \{c_m^\dagger c_n + c_n^\dagger c_m\}, \tag{1}$$

where the hopping amplitude t sets the energy scale. The sum runs over nearest-neighbor bonds, with m and n representing sites at the end of each bond. The operator $c_m^\dagger$ creates a particle at site m, while c_n annihilates a particle at site n. The Hamiltonian can be viewed as encoding time evolution on a discrete graph. A particle that is initially localized at one site can hop to the immediate neighbors in one step. Upon repeated action of the Hamiltonian, the particle may hop onto the next-nearest neighbors and further.

The geometry of the space is encoded in the assignment of neighbors. Away from the singularity, each site has $2D$ neighbors, where D is the dimensionality of the surface. As shown in Fig. 1, the singularity is a single site with $(2MD)$ neighbors, where M is the degree of the singularity; we have $2D$ neighbors per surface, with M surfaces in total. Operationally, we take each surface to have linear dimension L with periodic boundaries. The total number of sites in the problem is then $N = ML^D - M + 1$. The resulting Hamiltonian is an $N \times N$ symmetric matrix. Its eigenvectors represent stationary states, while the eigenvalues yield the corresponding energies. For small system sizes, we carry out full diagonalization to find all eigenvectors and eigenvalues. For large systems, we take advantage of the sparse character of the tight-binding Hamiltonian and employ Krylov-space-based routines to find the lowest few eigenstates.

In the tight-binding setup, an eigenstate satisfies the following relation at every site:

$$-t \sum_{m(n)} \psi_m = E \psi_n, \tag{2}$$

where n represents any given site. The index $m(n)$ runs over the neighbors of n, ψ_p represents the eigenvector component at site p, and E represents the eigenvalue.

A bound state can be identified in two ways: from the eigenvector or from the eigenvalue. The eigenvector must be peaked at the singularity, decaying to zero as we move away. The eigenvalue must lie below a threshold value, $-2Dt$, representing the lowest value possible for a delocalized state on a D-dimensional surface. This can be expressed in terms of a binding energy, $E_{\text{binding}} = -2Dt - E_{\text{state}}$. A bound state must have a positive binding energy. The higher the binding energy is, more bound the state is.

For the one-dimensional tight-binding problem with a setup as shown in Fig. 1 (left), the bound state(s) can be found using analytic arguments. They are exponentially localized around the singularity, as we show below. More generally, the eigenvalues and eigenvectors can be found numerically.

III. $D = 1$: INTERSECTING WIRES

A. Analytic solution to the tight-binding problem

We first discuss the case of M one-dimensional wires intersecting at a pointlike junction. The arguments in this section were first presented in Ref. [15] in the context of a certain magnetic model. To represent the wave function, we denote the junction site as $j = 0$. To all other sites, we assign an integer value that encodes distance from the junction. For example, the immediate neighbors of the junction are assigned $j = 1$. This tight-binding problem produces one bound eigenstate, described by the ansatz

$$\psi_j = \frac{1}{\mathcal{N}} e^{-\alpha_M j}, \quad \psi_0 = \frac{1}{\mathcal{N}}. \tag{3}$$

Here, $\mathcal{N}$ is a normalization constant. We demand that it be an eigenstate with eigenvalue E_M. At a site away from the junction, the eigenstate condition of Eq. (2) yields

$$-t(e^{-\alpha_M} + e^{\alpha_M}) = E_M. \tag{4}$$

At the junction site, the same condition yields

$$-2Mte^{-\alpha_M} = E_M. \tag{5}$$

From Eqs. (4) and (5), we solve for α_M and E_M,

$$\alpha_M = \tfrac{1}{2}\ln\{2M-1\}, \quad E_M = -2Mt/\sqrt{2M-1}. \tag{6}$$

Note that for $M = 1$, there is no singularity because we have only one wire. In this limit, the bound state vanishes as $\alpha_{M=1} = 0$ and $E_{M=1} = -2t$. For $M \geqslant 2$, α_M represents a decay constant. The binding energy is given by $E_{\text{binding},D=1} = (-2t - E_M)$. The normalization constant can be explicitly found, $\mathcal{N} = \sqrt{\frac{2M-1}{M-1}}$.

For $M \geqslant 2$, α_M monotonically increases with M. In parallel, E_M monotonically decreases, or equivalently, the binding energy monotonically increases. This shows that the state becomes progressively more bound as the degree of the singularity increases. For very large M, the bound state is entirely localized at the singularity.

B. Comparison with bound states induced by a potential

The bound state at the singularity can be compared to one induced by a local attractive potential. Within the tight-binding approach, we consider a smooth one-dimensional chain with sites labeled by j, a coordinate that runs over all integers. At $j = 0$, we have an on-site attractive potential of strength g. The Hamiltonian is given by

$$H_{1\text{D},g} = -t\sum_j \{c_j^\dagger c_{j+1} + c_{j+1}^\dagger c_j\} - g c_0^\dagger c_0. \tag{7}$$

This problem also generates a bound state, with the wave function

$$\psi_j = \frac{1}{\mathcal{N}'} e^{-\alpha_g |j|}, \tag{8}$$

where $\mathcal{N}'$ is a normalization constant. For $j \neq 0$, the eigenstate condition takes the same form as Eq. (4). At $j = 0$, the condition is modified by the potential to give

$$-2te^{-\alpha_g} - g = E_g, \tag{9}$$

where E_g is the eigenvalue. It is convenient to express the potential strength and the energy eigenvalue as dimensionless quantities, using $\tilde{g} \equiv g/2t$ and $\tilde{E}_g = E_g/2t$. In terms of these quantities, we find

$$\alpha_g = \ln\{\tilde{g} + \sqrt{\tilde{g}^2+1}\}, \quad \tilde{E}_g = \frac{-\tilde{g}^2 - \tilde{g}\sqrt{\tilde{g}^2+1} - 1}{\tilde{g} + \sqrt{\tilde{g}^2+1}}. \tag{10}$$

The normalization constant comes out to be $\mathcal{N}' = \sqrt{1 + \frac{1}{\tilde{g}\{\tilde{g}+\sqrt{\tilde{g}^2+1}\}}}$. These values describe a bound state induced by a potential on a smooth one-dimensional space with no singularities. In contrast, those in Eq. (6) describe a bound state created at a singularity of codimension 1 and degree M, with no potential involved. Remarkably, the wave functions have the same form in both cases as given by Eqs. (3) and (8). This allows us to draw a precise equivalence, $M \leftrightarrow \tilde{g}_M$, where $\tilde{g}_M$ satisfies

$$M = \left[\tilde{g}_M^2 + \tilde{g}_M\sqrt{\tilde{g}_M^2+1} + 1\right]. \tag{11}$$

The equivalence can be stated as follows. On the one hand, we consider a singularity of codimension 1 and degree M, with no potential. On the other hand, we consider a potential of strength $\tilde{g}_M$ on a smooth one-dimensional chain. These two situations produce bound states with precisely the same decay constant *and* binding energy.

The equivalent potential $\tilde{g}_M$ increases monotonically with M. For large M, we see that $\tilde{g}_M \sim \sqrt{M}$.

C. Mechanism for binding

A bound state has lower energy than the continuum of delocalized states. The underlying mechanism provides some way for the bound state to lower its energy. What is the mechanism in the case of a potential or in the case of a singularity? This question can be directly addressed within the tight-binding approach where the Hamiltonian is a sum of local terms. We have one term for each bond, representing the kinetic energy of hopping between two sites. In the case of a potential, we also have an on-site potential energy. Given the ground-state wave function, we may evaluate the contribution of each term to its energy.

For the case of a potential-induced bound state, the Hamiltonian is given by Eq. (7) with the wave function given by Eq. (8). Bound-state formation is driven by the potential-energy term. This can be seen by examining the potential-energy contribution as a fraction of the bound state's energy,

$$\frac{\langle -gc_0^\dagger c_0\rangle}{E_g} = \left(\frac{\tilde{g}^2 + \tilde{g}\sqrt{\tilde{g}^2+1}}{\tilde{g}^2 + \tilde{g}\sqrt{\tilde{g}^2+1} + 1}\right)^2 = \left(\frac{-\tilde{g}}{\tilde{E}_g}\right)^2. \tag{12}$$

For very small $\tilde{g}$, this quantity approaches zero. This is because the state is well spread with low weight at the potential. At $\tilde{g} = 1$, it becomes $\frac{1}{2}$. For large $\tilde{g}$, it approaches unity; the energy of the bound state comes almost entirely from the potential-energy term. This reveals that the mechanism for bound-state formation is potential energy lowering.

We now make a comparison with the case of a bound state at a singularity. The Hamiltonian can be written in the form of Eq. (1) with the wave function given by Eq. (3).

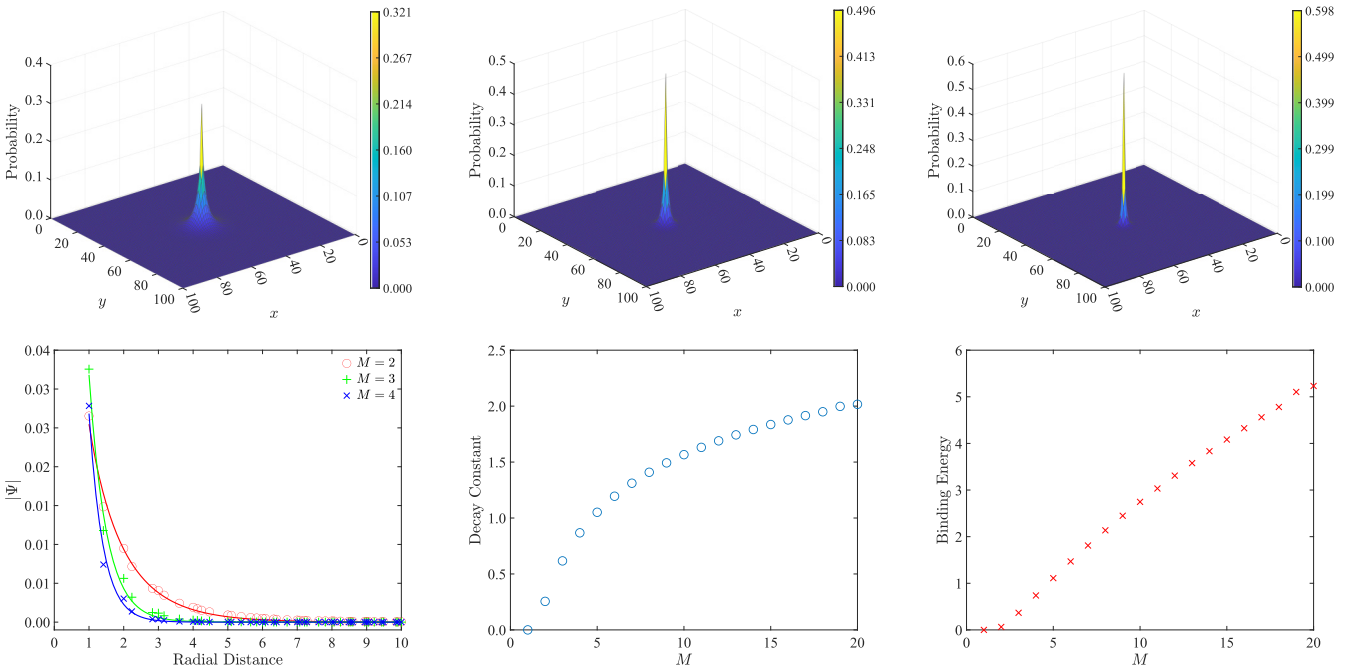

FIG. 2. The ground state on a space with M 2D sheets intersecting at a point. The plots correspond to $M = 2$ (top left), $M = 3$ (top middle), and $M = 5$ (top right). Each 2D sheet is taken to be a 100×100 grid with periodic boundaries. The origin is common to all the sheets. The plots show the spatial variation in the probability (amplitude squared). These wave functions fit well to a modified Bessel form of order 0 (bottom left). As the degree of the singularity increases, the decay constant obtained from the fit increases (bottom middle), as does the binding energy (bottom right). The binding energy is shown in units of t.

Binding is driven by the M bonds that connect outward from the singularity. We evaluate

$$\frac{-t\sum_{j(0)}\langle\{c_j^\dagger c_0 + c_0^\dagger c_j\}\rangle}{E_M} = \frac{2M-2}{2M-1}. \tag{13}$$

The index $j(0)$ runs over the $2M$ sites that are directly connected to the singularity. When $M = 1$, this ratio vanishes because we have a delocalized ground state. For $M = 2$, this ratio yields $2/3$, i.e., two thirds of the ground-state energy arises from the immediate vicinity of the singularity. For large M, this ratio approaches unity. That is, all of the ground state's energy comes from the $2M$ bonds that are connected to the junction. This represents a kinetic-energy contribution, arising from the particle's "shuttling" motion from one wire to another. This is a new form of kinetic energy that is not present on smooth surfaces. The ground state is bound due to shuttling kinetic energy that can be gained only in the vicinity of the singularity.

IV. $D = 2$: INTERSECTING SHEETS

We next consider singularities of codimension 2, with an example shown in Fig. 1 (middle). We consider the space of M sheets that share a common point. We discretize the space using a square grid for each sheet, assuming that they intersect at the origin. This setup generates a single bound state for any $M \geqslant 2$. However, the wave function cannot be expressed as a simple analytic form. Instead, we present numerical solutions and fit them to a suitable functional form.

A. Numerical solution to the tight-binding problem

We consider M sheets, each modeled as an $L \times L$ square grid. The sheets may have open or periodic boundaries. A generic point in this system has four nearest neighbors, as it lies on a two-dimensional sheet. In contrast, the central point in every sheet is taken to be the same. This point has $4M$ neighbors, four on each of the M sheets. This configuration defines a graph with $\{ML^2 - (M-1)\}$ sites. We solve the tight-binding Hamiltonian of Eq. (1) on this graph by numerical diagonalization. We identify the lowest eigenstate and examine its wave function. As we show below, this state decays rapidly as we move away from the center point. As it decays before reaching the boundaries, it is not sensitive to boundary conditions.

Figure 2 (top row) shows examples of the bound-state wave function. It plots the squared amplitude, the probability of finding the particle at each site. The panels, from left to right, correspond to $M = 2, 3$, and 5. In each case, the wave function on one of the intersecting sheets is shown; the same wave function appears on every sheet. From the plots, we immediately see localized character, with probability peaking at the singularity and decaying as we move away. With increasing degree of the singularity (increasing M), the ground state becomes more tightly bound.

The same information is shown as a two-dimensional plot in Fig. 2 (bottom left), with the wave-function amplitude plotted against the radial coordinate (distance from the singularity). The solution has circular symmetry: sites with the same radial coordinate have the same wave-function amplitude. Note that the phase is uniform at all points. As shown in

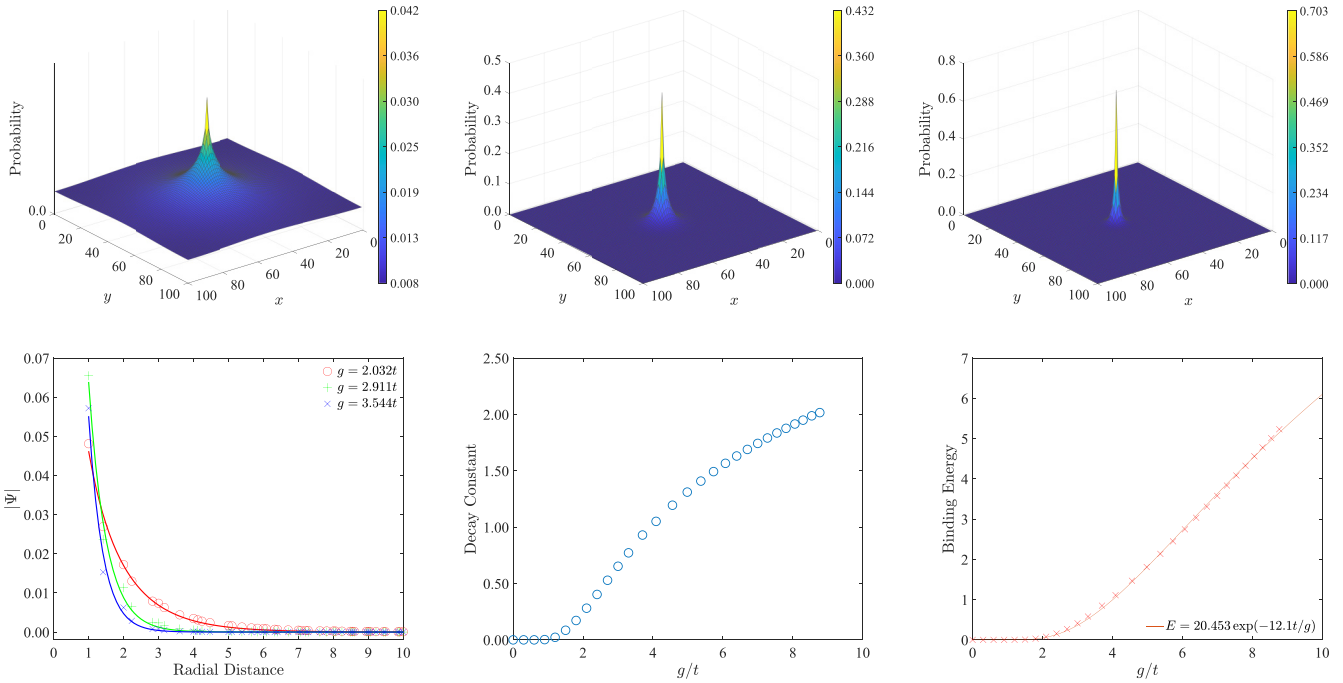

FIG. 3. The ground-state wave function on a 2D sheet with an on-site attractive potential. The panels on top correspond to $g = t$ (left), $g = 2.032\,t$ (middle), and $g = 2.911\,t$ (right). They show the spatial variation of the probability (amplitude squared). The 2D sheet is taken to be a 100×100 grid with periodic boundaries. The wave-function profile is shown in the bottom left panel, with the amplitude plotted against the radial coordinate. The data are fit to modified Bessel functions of order 0. In the bottom middle panel, we plot the decay constant vs g. In the bottom right panel, we plot the binding energy (in units of t) vs the strength of the potential. The best-fit curve to the form $E_{\text{binding}} = Ae^{-B/g}$ is shown.

Fig. 2 (bottom left), the amplitude is well fit by a function of the form

$$f(r) = a\,k_0(\gamma r + b). \tag{14}$$

Here, k_ν is the modified Bessel function of the second kind, of order ν. This form is known from the continuum problem of a bound state induced by an attractive local potential in two dimensions, e.g., a square-well potential (see Refs. [18,19]). The bound wave function takes this form in the external region (outside the well). For each value of M, we obtain a, b, and γ as fitting parameters. The coefficient b represents a horizontal shift. For any $M \geqslant 2$, the best-fit value of b is less than the lattice spacing. The quantity γ encodes a horizontal stretch. It can be viewed as a decay constant—the higher the value of γ is, the more tightly bound the wave function is. As shown in Fig. 2 (bottom middle), γ increases monotonically with M. Finally, Fig. 2 (bottom right) shows the binding energy vs M. This encodes the energy difference between the bound state and the lowest delocalized state ($E_{\text{min.delocalized,2D}} = -4t$). As M increases, the binding energy increases. This supports the contention that the ground state becomes more tightly bound.

We summarize these findings as follows. A bound state is formed for any singularity of codimension 2. The higher the degree of the singularity is, the more tightly bound the state.

B. Comparison with bound states induced by a potential

For comparison, we consider a smooth two-dimensional surface with a local attractive potential. The Hamiltonian for this system is similar to Eq. (7). We have a single $L \times L$ sheet with an attractive potential of strength g at the central site. Analytic solutions cannot be found, but a single bound state is seen in the numerics for any attractive potential. If the system size is large enough, the wave function decays to zero at the boundaries. As a result, the ground state is not sensitive to boundary conditions. We describe this state below and compare it with the continuum problem of a local attractive potential in two dimensions [18].

Figure 3 (top) shows the bound-state wave function for $g/t = 1,\ 2.032$, and 2.911. The latter two values are chosen as they are equivalent to singularities with $M = 2$ and 3, respectively, as we discuss below. We emphasize that any value of g produces a similar ground state. Figure 3 (bottom left) shows the same wave functions, fitted to the form given in Eq. (14). We find good agreement with the Bessel function form, especially at large distances. As shown in the bottom middle and right panels of Fig. 3, the decay constant γ and the binding energy increase monotonically with g. The larger the potential is, the tighter the bound state is. For small g, the binding energy is exponentially weak. As shown Fig. 3, the dependence on g is well fit by the function $E_{\text{binding}} = Ae^{-B/g}$. This form is known from the continuum problem of a bound state induced by a local potential (say, of the δ-function form). For example, it is invoked in the discussion of the Cooper instability [26,27], where electron pairs that are constrained to live on a two-dimensional space experience a weak attraction.

We now compare bound states induced by singularities with those induced by potentials. We treat M and g as

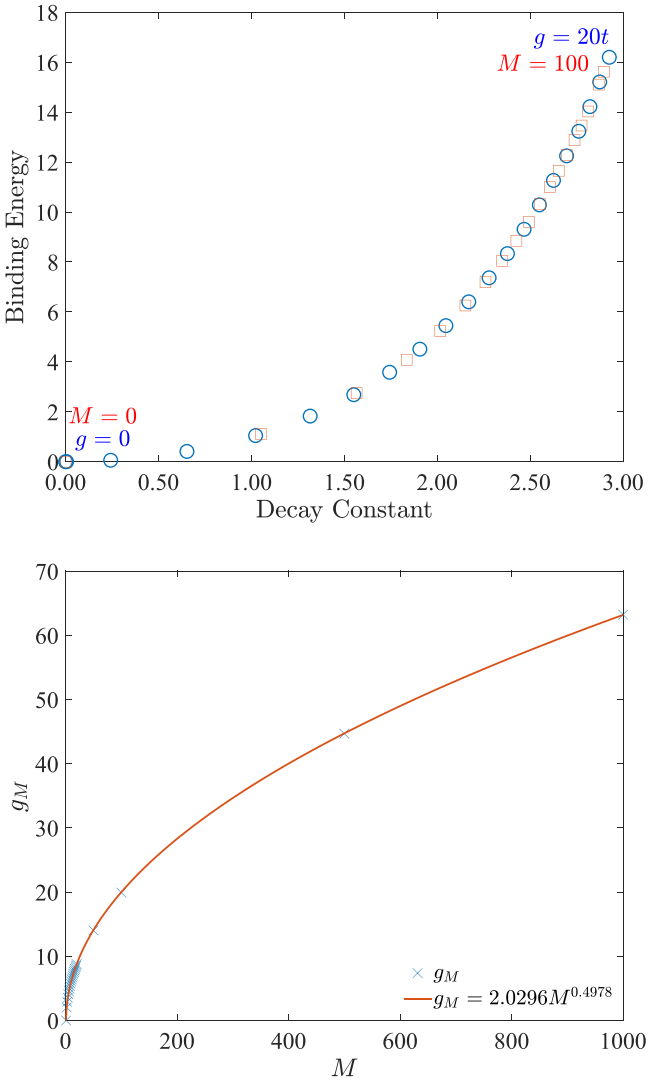

FIG. 4. Top: Binding energy vs decay constant in two dimensions. Blue circles represent bound states induced by a local potential on a smooth two-dimensional sheet. From left to right, the points correspond to increasing potential strength, with g increasing from 0 to $20t$ in steps of t. Red squares represent bound states induced by singularities of codimension 2. From left to right, the degree of the singularity M increases in steps of 5 from 0 to 100. The two data sets collapse onto the same curve. Bottom: g_M vs M, where g_M is the potential that is equivalent to a singularity of degree M. The data fit well to a function of the form $g_M \sim \sqrt{M}$.

tunable handles in the two cases. In both, we obtain localized ground states that fit well to the same functional form. In gross terms, the solutions are described by two parameters: the decay constant and the binding energy. These are both monotonically increasing functions of the tuning handle in each case. Remarkably, they are not independent. The decay constant immediately determines the binding energy and vice versa. This is shown in Fig. 4, which plots the binding energy vs decay constant for both singularity-induced and potential-induced bound states. The data points collapse onto the same curve. This leads us to conclude that potentials and singularities lead to the same bound states. For a singularity of degree M, we can find an equivalent potential g_M that generates a bound state with the same decay constant and binding energy. Figure 3 (bottom right) shows the variation in g_M with M. As M increases, the equivalent potential grows in strength. For large M, we find $g_M \sim \sqrt{M}$.

We have verified that the equivalence goes beyond the decay constant and binding energy. It holds even for the precise form of the wave function, up to a change in the normalization to account for multiple sheets.

V. $D = 3$: INTERSECTING THREE-DIMENSIONAL SPACES

We proceed to singularities of codimension 3, with an example shown in Fig. 1 (right). As with codimension 2, analytic solutions cannot be found. We present numerical solutions and fit them to functional forms that are inspired by the continuum problem.

A. Numerical solution to the tight-binding problem

We consider M three-dimensional (3D) spaces that share a common point. We discretize each space using an $L \times L \times L$ cubic grid. The central point is taken to be common to all spaces. While a generic point has six neighbors, the center has $6M$ neighbors. This configuration defines a graph with $\{ML^3 - (M-1)\}$ sites. We solve the tight-binding Hamiltonian of Eq. (1) on this graph numerically. We examine the energy and wave function of the lowest eigenstate. If a state is bound and L is large enough, the wave function will decay before reaching the boundaries. The wave function will then be indifferent to open or periodic boundary conditions.

The codimension-3 solutions present a remarkable difference when compared with codimensions 1 and 2. A bound state forms only when the degree of the singularity exceeds a threshold value. For example, as shown in Fig. 5 (left), we find no bound state for $M = 3$ (three cubes intersecting a point). However, there is a clear bound state when $M = 5$ (five cubes intersecting at a point), as shown in Fig. 5 (right). This can be seen in various ways, as we describe below. We first note that any such analysis requires a systematic approach to the thermodynamic limit by increasing L. A true bound state will remain bound with a constant "width" as L increases. In contrast, a delocalized state will expand with increasing system size.

We introduce a quantitative measure for localization,

$$r_{\text{avg}} = \sum_j |\vec{r}_j - \vec{r}_0| \times |\psi_{j,0}|^2, \tag{15}$$

where j runs over all sites in the tight-binding setup. The distance between the origin and site j is denoted as $|\vec{r}_j - \vec{r}_0|$. Note that distances are calculated as on the usual cubic lattice: a point with coordinates (x, y, z) is at a distance of $\sqrt{x^2 + y^2 + z^2}$ from the origin. The probability amplitude of the *ground state* at this site is denoted as $|\psi_{j,0}|$. Assuming that the particle resides in the ground state, r_{avg} denotes its average separation from the singularity. If the ground state represents a true bound state, r_{avg}/L will extrapolate to zero as $L \to \infty$. Instead, if the ground state is delocalized, r_{avg}/L will extrapolate to a nonzero value. Figure 5 (bottom left)

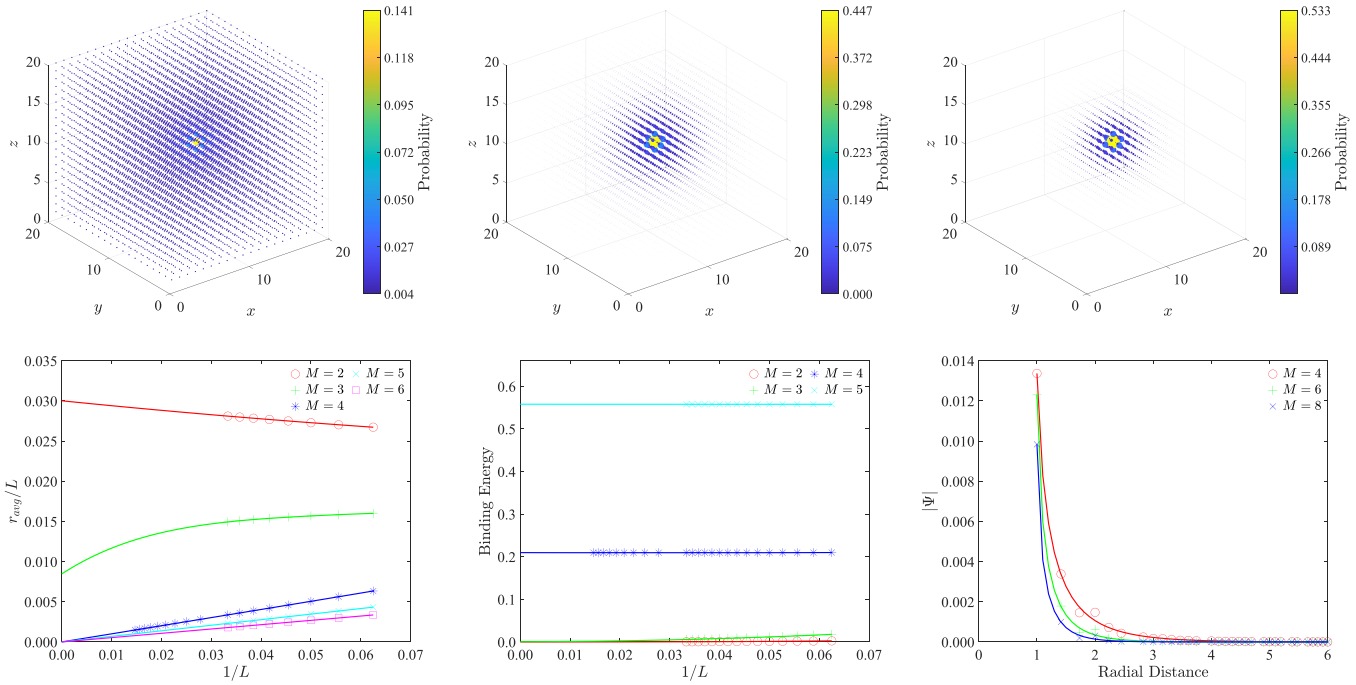

FIG. 5. The ground state of a particle on a space of M cubes intersecting at a point, where $M = 3$ (top left), $M = 4$ (top middle), and $M = 5$ (top right). Each cube is taken to be a $20 \times 20 \times 20$ grid with periodic boundaries. The center point is shared by all cubes, representing a point of intersection. In each plot, both the size and color of the markers represent the same quantity. They encode the probability of finding the particle (amplitude squared) at a certain site. We show only sites on a single cube because the wave function is the same across cubes. In the bottom left panel, we plot r_{avg}/L vs $1/L$ (see text). The data are fit to the form $y = a + b/L + c/L^2$ in order to extrapolate to $L \to \infty$. In the bottom middle panel, we plot the binding energy vs $1/L$ with fits to the form $y = a + b/L + c/L^2$. Finally, in the bottom right panel, we plot the wave-function amplitude against the radial coordinate for $M = 4, 6, 8$. The data are fit to a modified Bessel form (see text).

compares r_{avg}/L vs $1/L$ for various M values. We see a qualitative shift between $M = 3$ and $M = 4$, with $M \geqslant 4$ showing bound-state formation.

We next examine the binding energy. It is defined as the energy separation between the lowest state and the bottom of the delocalized continuum ($E_{\text{min.delocalized,3D}} = -6t$). If the ground state is truly bound, E_{binding} will approach a nonzero value as $L \to \infty$. In a delocalized state, E_{binding} will vanish for large L. Figure 5 (bottom middle) shows E_{binding} vs $1/L$ for various M values. Once again, we find behavior that is consistent with bound-state formation only when $M \geqslant 4$.

To characterize the wave function in a systematic manner, we fit it to the form

$$h(r) = c\, r^{-1/2} k_{1/2}(\gamma r + b). \tag{16}$$

Here, $k_{1/2}$ represents a modified Bessel function of the second kind of order 1/2. This form is known from the continuum problem of a 3D attractive square well. When a bound state is produced, its wave function follows this form in the external region (outside the well) [18,19]. We find a good fit to the modified Bessel form as long as $M \geqslant 4$, as shown in Fig. 5 (bottom right). The wave-function amplitude at each site depends solely on the radial distance from the singularity. The phase is ignored as it is uniform at all sites.

From the fit, we obtain the decay constant γ. For $M \geqslant 4$, the decay constant increases with increasing M, as does the binding energy, as we discuss below. The ground state becomes progressively more bound.

B. Comparison with bound states induced by a potential

Like before, we compare our results with a smooth three-dimensional surface with a local attractive potential. We model this as a tight-binding problem on an $L \times L \times L$ cubic grid. We place an attractive on-site potential of strength g at the center. For small values of g, the ground state is not localized. A bound state is formed only when g exceeds a threshold value. The ground state is plotted in the top panels of Fig. 6 for $g = 4t$, $4.657t$, and $5.246t$. The first clearly shows a delocalized ground state, while the latter two are bound. In fact, we will argue below that the latter two values are equivalent to $M = 4$ and 5.

We approach the question of bound-state formation in the same manner as for the singularity above. The bottom left and middle panels of Fig. 6 show r_{avg}/L and the binding energy vs $1/L$ for a few potential strengths. We see two clear regimes, $g \lesssim 4t$ and $g \gtrsim 4.05t$. In the former, r_{avg}/L extrapolates to a nonzero value as $L \to \infty$. At the same time, the binding energy extrapolates to zero. In the latter, r_{avg}/L extrapolates to zero, while the binding energy extrapolates to a nonzero value. This suggests a threshold value, g_{critical}, that separates bound and unbound behavior. This result is the tight-binding analog of a well-known result in quantum mechanics: in three

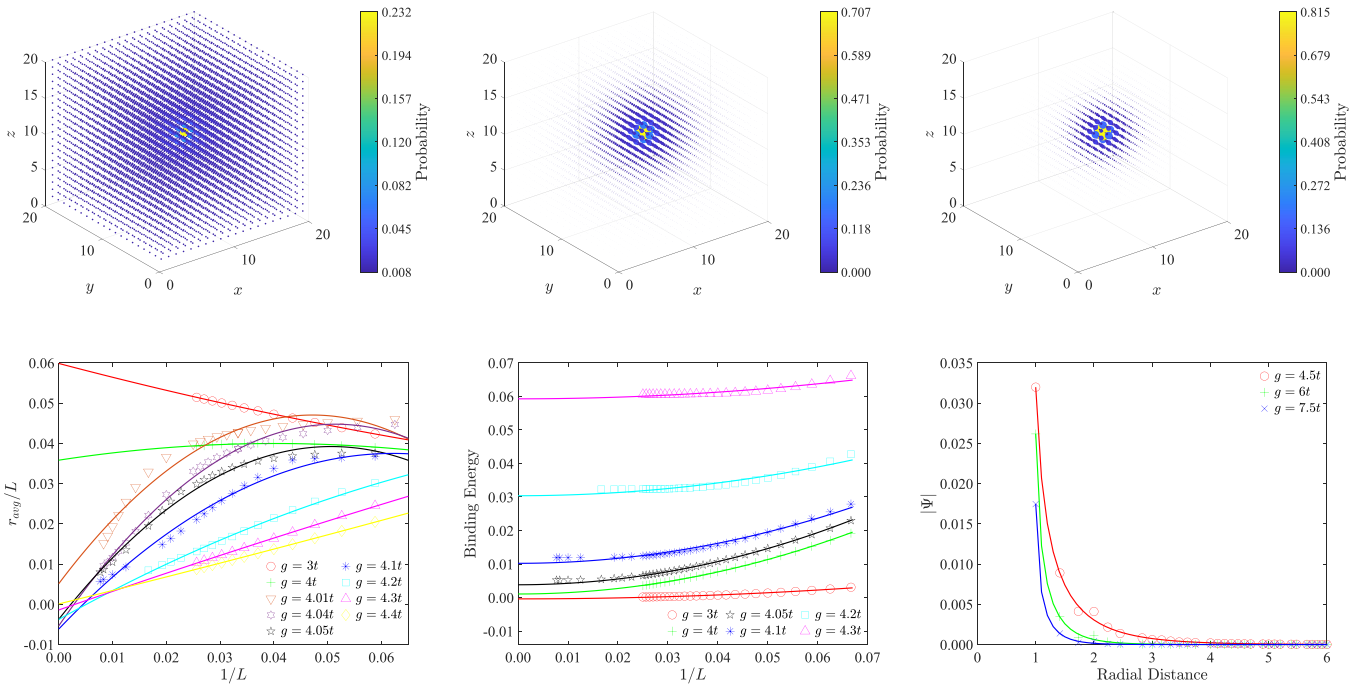

FIG. 6. The ground state on a 3D space with a local attractive potential. The panels on top correspond to $g = 4\,t$ (left), $g = 4.657\,t$ (middle) and $g = 5.246\,t$ (right). The space is taken to be a $20 \times 20 \times 20$ cubic grid with periodic boundaries with the on-site potential at the center. In each plot, the size and color of the markers represent the probability of finding the particle (amplitude squared) at a certain site. In the bottom left panel, we plot r_{avg}/L vs $1/L$ for various potential strengths. The data are fit to the form $y = a + b/L + c/L^2$. In the bottom middle panel, we plot the binding energy (see text) vs $1/L$, with fits to the form $y = a + b/L^2$. In the bottom right panel, the wave-function amplitude is plotted as a function of the radial distance from the potential. The data are fit to a modified Bessel function form (see text).

dimensions, a critical potential strength is required for bound-state formation.

The precise location of the critical point is difficult to pinpoint due to system-size limitations. For example, near the transition, the fitting curves to r_{avg}/L vs $1/L$ cannot be reliably extrapolated to $1/L \to 0$ within accessible system sizes. The binding-energy curves in Fig. 6 (bottom middle) are somewhat clearer: g_{critical} appears to lie between $g = 4.00t$ and $4.05t$.

Figure 6 (bottom left) shows the evolution of r_{avg}/L with g. We see a qualitative change between two regimes, one where r_{avg}/L extrapolates to zero as $L \to \infty$ and one where it tends to a nonzero value. The boundary between these regimes cannot be precisely discerned within accessible system sizes. In Fig. 6 (bottom middle), we see the evolution of binding energy with system size for various values of g. Based on the values extrapolated to $L \to \infty$, we conclude that the critical potential strength lies between $g = 4.00t$ and $4.05t$. Figure 6 (bottom left) shows the evolution of r_{avg}/L with g.

When the potential exceeds g_{critical}, the resulting bound state fits well to the modified Bessel form of Eq. (16). This is shown in Fig. 6 (bottom right). The best-fit value of the decay constant γ increases monotonically with increasing g. Likewise, the binding energy increases with g. A bound state forms when g exceeds g_{critical}, becoming progressively more bound as g increases further. We now compare results for a singularity with those for a potential. Bound states fit well to the same analytic form in both cases. As with the two-dimensional case, the decay constant and the binding energy are not independent. Figure 7 (top) plots the variation of these two parameters for singularity-driven and potential-driven bound states. Data from both cases collapse onto a single curve. This brings out a quantitative equivalence between singularities and potentials. For a singularity of degree M, we assign an equivalent potential g_M. The degree-M singularity produces a bound state with the same decay constant and binding energy as an attractive potential of strength g_M. Figure 7 (bottom) shows a plot of g_M vs M. For large M, g_M approximately scales as $\sqrt{M}$. The equivalence is not restricted to the decay constant and binding energy. We have verified that it holds for the precise forms of the wave function, up to a change in the normalization constant.

VI. DISCUSSION

We have demonstrated that singularities arising from intersections produce bound states in the same way as attractive potentials. This mapping is quantitative in nature, where each singularity can be assigned an effective potential strength. In singularities, the binding mechanism is the kinetic energy of shuttling, where the particle moves back and forth across surfaces. This can be viewed as "quantum indecision"—the particle remains frozen at a crossroads as it is unable to pick a direction of propagation. A bound state allows the system to sample all surfaces to small distances while rapidly shuttling among surfaces. This notion can be tested in semiconductor architectures [28], ultracold atomic gases [29] and superconducting circuits [30].

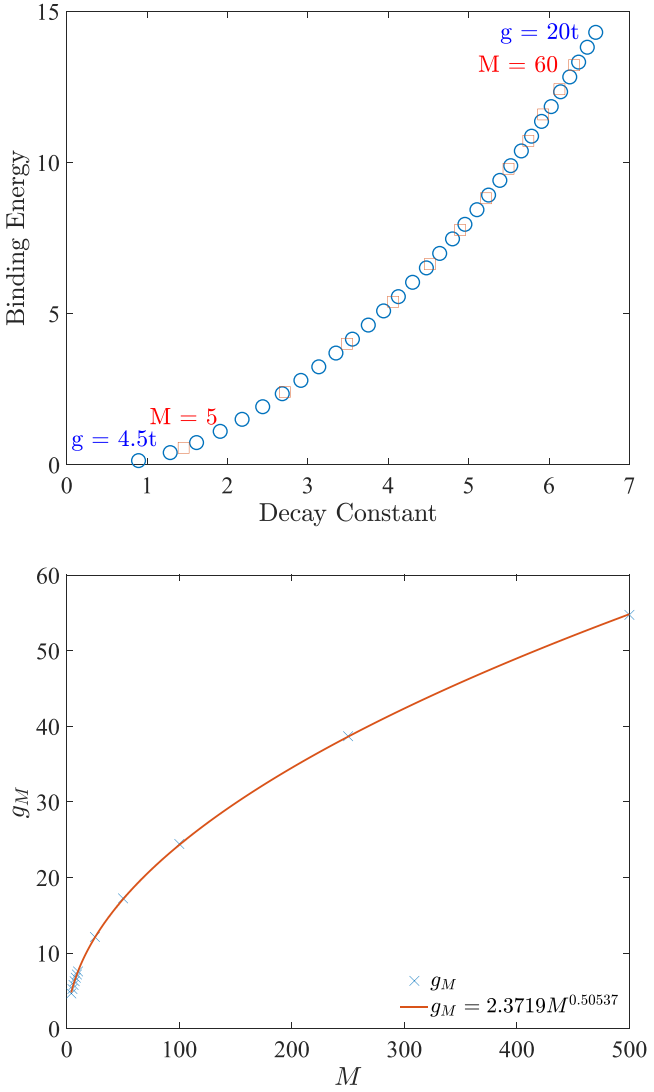

FIG. 7. Top: Binding energy vs decay constant in three dimensions. Blue circles represent bound states induced by a local potential. From left to right, points correspond to increasing potential strength, with g increasing from $4.5t$ to $20t$ in steps of $0.5t$. Red squares represent bound states induced by singularities of codimension 3. From left to right, the degree of the singularity M increases in steps of 5 from 5 to 60. The two data sets collapse onto the same curve. Bottom: g_M vs M, where g_M is the potential that is equivalent to a singularity of degree M.

We have focused on a class of spaces where the singularity is zero-dimensional, i.e., where smooth spaces intersect at a point. Within this class, the key factor that determines bound-state formation is the dimensionality of the spaces involved. Our results can be generalized to higher-dimensional singularities, with the key factor being codimensionality—the difference in dimensionality between the smooth spaces and the singularity. For example, consider two 2D sheets that intersect along a line. In this case, we have translational symmetry along the intersection line. This generates a new conserved quantity—momentum along the intersection line. For each value of this momentum, we are left with an effective problem of two lines that intersect at a point. We conclude that a bound state can form for each momentum. All of these states may not be truly bound. If the kinetic energy of motion along the intersection line exceeds the binding energy, this state can scatter and delocalize. An example of this physics is discussed in Sec. IX of Ref. [12].

Our results regarding the role of dimensionality in bound-state formation are particularly relevant to quantum magnets. In the presence of frustration, the low-energy physics of a magnet resembles a particle moving on an abstract space [12,13]. When this space self-intersects, the particle localizes. This manifests as magnetic ordering in a particular classical configuration. Codimension-1 singularities have been found and argued to host bound states [12,14,15]. Codimension-3 singularities have been found and argued *not* to host bound states [13,31]. Building on these results, magnetic clusters can be designed to simulate spaces with multiple wires, sheets, or even three-dimensional spaces. The Kitaev spin-S chain serves as an example, with classical ground states that form a networklike space. Each node of the network is an intersection of M wires, where M can be tuned by changing the length of the chain [15].

The analogy between singularities and potentials highlights the role of dimensionality in bound-state formation. In higher dimensions, the tendency of a particle to spread is stronger because the space available for spreading is larger. As a result, a stronger potential or a singularity of higher degree is required. A similar idea is invoked in Anderson localization [32,33]. In one or two dimensions, an infinitesimal amount of disorder suffices to localize a particle. However, a threshold disorder strength is required in three and higher dimensions. This has been related to the problem of a random walker and the mean time spent in a neighborhood [34]. The higher the dimensionality is, the shorter the time spent in a neighborhood is. The particle may show localizing tendencies, which, upon quantization, manifest as bound states.

We have based our arguments on a tight-binding framework where potentials and intersections can be handled on the same footing. More generally, the same problem can also be addressed in the continuum. There is extensive literature on quantum graphs where eigenfunctions of the Schrödinger operator can be found on each link, with suitable boundary conditions enforced at junctions. Studies have explored various choices for boundary conditions and their consequences [22,35,36]. Reference [37] compared the traditional quantum graph approach with tight binding (assuming plane-wave-like unbound states). With continuum problems on open or singular spaces, a careful self-adjoint formulation can give rise to bound states [38]. Our results pose an interesting question for future studies: what are the boundary conditions in the continuum problem that reproduce the tight-binding bound state?

ACKNOWLEDGMENTS

We thank D. Sen, K. Samokhin, J.-S. Bernier, S. Khatua, and A. Soori for insightful discussions. We thank E. Tan for discussions on technical aspects. This work was supported by the Natural Sciences and Engineering Research Council of Canada.

[1] F. Sols, M. Macucci, U. Ravaioli, and K. Hess, J. Appl. Phys. **66**, 3892 (1989).

[2] K.-F. Berggren and Z.-L. Ji, Phys. Rev. B **43**, 4760 (1991).

[3] Z.-L. Ji and K.-F. Berggren, Phys. Rev. B **45**, 6652 (1992).

[4] P. Exner, P. Šeba, M. Tater, and D. Vank, J. Math. Phys. **37**, 4867 (1996).

[5] R. L. Schult, D. G. Ravenhall, and H. W. Wyld, Phys. Rev. B **39**, 5476 (1989).

[6] Y. B. Gaididei, L. I. Malysheva, and A. I. Onipko, J. Phys.: Condens. Matter **4**, 7103 (1992).

[7] A. R. Goñi, L. N. Pfeiffer, K. W. West, A. Pinczuk, H. U. Baranger, and H. L. Stormer, Appl. Phys. Lett. **61**, 1956 (1992).

[8] J. Hasen, L. Pfeiffer, A. Pinczuk, H. Baranger, K. West, and B. Dennis, Superlattices Microstruct. **22**, 359 (1997).

[9] E. N. Bulgakov, P. Exner, K. N. Pichugin, and A. F. Sadreev, Phys. Rev. B **66**, 155109 (2002).

[10] D. N. Maksimov and A. F. Sadreev, Phys. Rev. E **74**, 016201 (2006).

[11] S. Nakarmi, V. U. Unnikrishnan, V. Varshney, and A. K. Roy, Front. Mater. **8**, 692988 (2021).

[12] S. Khatua, D. Sen, and R. Ganesh, Phys. Rev. B **100**, 134411 (2019).

[13] S. Khatua, Ph.D. thesis, Institute of Mathematical Sciences, 2021.

[14] S. Srinivasan, S. Khatua, G. Baskaran, and R. Ganesh, Phys. Rev. Res. **2**, 023212 (2020).

[15] S. Khatua, S. Srinivasan, and R. Ganesh, Phys. Rev. B **103**, 174412 (2021).

[16] B. Simon, Ann. Phys. (NY) **97**, 279 (1976).

[17] K. Yang and M. de Llano, Am. J. Phys. **57**, 85 (1989).

[18] M. M. Nieto, Phys. Lett. A **293**, 10 (2002).

[19] G. Lapicki and S. Geltman, J. At., Mol., Opt. Phys. **2011**, 573179 (2011).

[20] J. Gratus, C. J. Lambert, S. J. Robinson, and R. W. Tucker, J. Phys. A **27**, 6881 (1994).

[21] V. Kostrykin and R. Schrader, J. Phys. A **32**, 595 (1999).

[22] F. M. Andrade, A. Schmidt, E. Vicentini, B. Cheng, and M. da Luz, Phys. Rep. **647**, 1 (2016).

[23] N. W. Ashcroft and N. D. Mermin, *Solid State Physics* (Holt, Rinehart and Winston, New York, 1976).

[24] T. Allison, O. Coskuner, and C. Gonzalez, *Metallic Systems: A Quantum Chemist's Perspective* (CRC Press, Boca Raton, FL, 2011).

[25] W. Harrison, *Elementary Electronic Structure*, rev. ed. (World Scientific, Singapore, 2004).

[26] L. N. Cooper, Phys. Rev. **104**, 1189 (1956).

[27] C. Esebbag, J. M. Getino, M. de Llano, S. A. Moszkowski, U. Oseguera, A. Plastino, and H. Rubio, J. Math. Phys. **33**, 1221 (1992).

[28] G. Bastard, *Wave Mechanics Applied to Semiconductor Heterostructures*, Monographies de physique (Editions de Physique, 1988).

[29] J. Zakrzewski, Acta Phys. Pol. B **38**, 1673 (2007).

[30] D. K. Weiss, W. DeGottardi, J. Koch, and D. G. Ferguson, Phys. Rev. Res. **3**, 033244 (2021).

[31] S. Khatua, R. Shankar, and R. Ganesh, Phys. Rev. B **97**, 054403 (2018).

[32] E. N. Economou and C. M. Soukoulis, Phys. Rev. B **28**, 1093 (1983).

[33] E. N. Economou, C. M. Soukoulis, and A. D. Zdetsis, Phys. Rev. B **30**, 1686 (1984).

[34] W. A. Berger, H. G. Miller, and D. Waxman, Eur. Phys. J. A **37**, 357 (2008).

[35] T. Kottos and U. Smilansky, Ann. Phys. (NY) **274**, 76 (1999).

[36] M. Znojil, Can. J. Phys. **90**, 1287 (2012).

[37] A. Aharony and O. Entin-Wohlman, J. Phys. Chem. B **113**, 3676 (2009).

[38] T. Jurić, Universe **8**, 129 (2022).